Published in final edited form as:
Am J Physiol Heart Circ Physiol. 2001 April ; 280(4): H1905–H1915.

Localized injury in cardiomyocyte network: a new experimental model of ischemia-reperfusion arrhythmias

ARA ARUTUNYAN[1], **DANIEL R. WEBSTER**[2], **LUTHER M. SWIFT**[1], and **NARINE SARVAZYAN**[1]

[1] Department of Physiology, Texas Tech University Health Sciences Center, Lubbock, Texas 79430

[2] Department of Cell Biology and Biochemistry, Texas Tech University Health Sciences Center, Lubbock, Texas 79430

Abstract

Localized injury in cardiomyocyte network: a new experimental model of ischemia-reperfusion arrhythmias. *Am J Physiol Heart Circ Physiol* 280: H1905–H1915, 2001.—We developed a new experimental approach to study the effects of local injury in a multicellular preparation and tested the ability of the method to induce reperfusion arrhythmias in cardiomyocyte monolayers. A small region of injury was created using geometrically defined flows of control and ischemia-like solutions. Calcium transients were acquired simultaneously from injured, control, and border zone cells using fluo 4. Superfusion with the injury solution rapidly diminished the amplitude of calcium transients within the injury zone, followed by cessation of cell beating. Reperfusion caused an immediate tachyarrhythmic response in ~17% of experiments, with a wave front propagating from a single cell or small cell cluster within the former injury zone. Inclusion of a gap junction uncoupler (1 mM heptanol) in the injury solution narrowed the functional border and sharply increased the number of ectopic foci and the incidence of reperfusion arrhythmias. The model holds a potential to reveal both micro-and macroscopic features of propagation, conduction, and cell coupling in the normal and diseased myocardium and to serve as a new tool to test antiarrhythmic protocols in vitro.

Keywords

cultured myocytes; calcium transients; ischemic border zone

The discovery that on cellular and subcellular levels cardiac conduction is essentially discontinuous represents a seminal advance in cardiac physiology (32,34). The discontinuous nature of cardiac conduction implies that the microscopic topology of gap junctions, nonlinear coupling of membranes of individual cells, and electrotonic interactions between connected cells can produce marked changes in the macroscopic electrical behavior. However, it is extremely difficult to understand events on a cellular level using the entire heart due to the complex anatomic arrangement of millions of muscle cells, the presence of fibrous tissue, and the resultant functional and electrical heterogeneity (29,40). On the other hand, it is not feasible to study intercellular interactions and impulse conduction using single isolated myocytes. Therefore, the advancement of experimental approaches that provide insights about cell-to-cell communication and patterns of impulse

---

Address for reprint requests and other correspondence: N. Sarvazyan, Dept. of Physiology, Texas Tech Univ. Health Sciences Center, 3601 Fourth St., Lubbock TX 79430 (phynas@ttuhsc.edu).

propagation during control and adverse conditions such as ischemia, acidification, or uncoupling is greatly anticipated (34). Such experimental models should also be useful as a testing ground for a variety of mathematical models, which have addressed discontinuous impulse propagation in excitable media (1,31,33), and for currently available and anticipated anti-arrhythmic drug protocols (14).

Isotropic two-dimensional cultures of cardiac cells represent the simplest type of structural organization of cardiac tissue. Understanding how arrhythmias are generated in such a network can provide important clues to the origins of ischemia-reperfusion-induced arrhythmias in more complex cardiac structures. In this paper, we describe an experimental setup that allows us to monitor spatiotemporal changes in beating behavior induced in myocyte monolayers by a local “ischemia”-like injury. Specifically, our original tasks were: *1*) to design a chamber that creates a stable and localized area of injury within a small network of cultured cells, *2*) to find effective experimental means to observe patterns of wave propagation during 1–2 h of continuous acquisition, and *3*) to describe rhythm disturbances induced by local injury in monolayers of cultured myocytes from neonatal rats.

MATERIALS AND METHODS

All experiments involving animals were performed according to the Institutional Committee on Animal Care and Use of the Texas Tech University Health Sciences Center, which follows federal and state guidelines. Results are expressed as means ± SE.

Chemicals

Collagenase II was obtained from Worthington (Freehold, NJ). Media and porcine trypsin were obtained from GIBCO-BRL (Grand Island, NY). Fluo 4-acetoxymethyl ester (AM) was purchased from Molecular Probes (Eugene, OR). Fetal bovine serum (FBS) and all other chemicals were purchased from Sigma Chemical (St. Louis, MO).

Myocyte isolation

Cardiomyocytes from 1- and 2-day-old Sprague-Dawley rats were obtained by a modified enzymatic digestion procedure (39). Hearts were removed, rinsed in a cold calcium- and magnesium-free Hanks’ buffered salt solution (CMF-HBSS), and minced into ~1-mm^3 pieces. Tissue chunks were incubated overnight at 2°C in CMF-HBSS containing 0.1 mg/ml trypsin. The next day, they were washed with CMF-HBSS and treated with 0.4 mg/ml soybean trypsin inhibitor. The tissue was then collected into Leibovitz’s medium containing 0.8 mg/ml collagenase II and shaken for 20 min at 37°C. The cells were then gently triturated, passed through a cell strainer to remove any undigested pieces, and centrifuged for 3 min at 17.5 *g*. The pellet was resuspended in Dulbecco’s modified essential medium (DMEM) supplemented with 10% FBS.

Cell plating and culture

The cells were preplated for 1 h to extract fibroblasts and endothelial cells, which attach more rapidly than myocytes. Unattached cells were then collected, counted, and plated in a culture dish containing 25-mm laminin-coated glass coverslips (10^5 cells/cm^2). Cells were then kept under standard culture conditions in DMEM, supplemented with 5% FBS, 10 U/ml penicillin, 10 μg/ml gentamicin, and 1 μg/ml streptomycin. On the third day after plating, the cells formed interconnected confluent networks that exhibited rhythmic spontaneous contractions and were used for an additional 3–4 days. To determine the purity of our cultures, cells were stained for sarcomeric myosin using primary antibodies (clone MF-20) from the Developmental Studies Hybridoma Bank (University of Iowa, Iowa City, IA) as described previously (39).

Cell loading with fluorescent indicator

Cells were loaded with the fluorescent calcium indicator during a 1-h incubation with 5 μM of the AM form of fluo 4 in Tyrode solution at room temperature. Superfusion solutions contained 0.25 μM of fluo 4-AM to maintain the intracellular dye concentration during extended experiments. Large amplitudes of the fluo 4 transients and the fact that traces were collected from large regions of interest ensured the absence of motion artifacts. Each spontaneous or stimulated action potential caused a contraction and was associated with a large increase in the cytosolic free Ca^{2+} concentration ($[Ca^{2+}]_i$) recorded as a fluo 4 transient. Monitoring of $[Ca^{2+}]_i$ transients as the means to record cell beating rate, wave front, and velocity of impulse propagation was successfully used in previous studies (4,16,37) that employed neonatal cardiac cells.

Experimental chamber

The experimental chamber used a stainless steel holder to mount a glass coverslip on the raised surface of a plastic holder, which contained two inlets and one outlet (Fig. 1). The polished sides of the chamber provided airtight contact with the coverslip, whereas the Plexiglas ceiling left a 300-μm open perfusion space. Superfusion solutions were driven by a multisyringe pump (Harvard Apparatus) loaded with 10- and 30-ml glass syringes. The syringe volume determined the flow rates within the chamber and the size of the injury zone (I-zone) (Fig. 1*C*). Inflow rates were 75 and 30 μl/min for the control and injury solutions, respectively. The stainless steel holder was mounted in a microincubator (Medical Systems) equipped with a Peltier controller, which provided a constant temperature inside the chamber (25°C). Two platinum electrodes were embedded into the top part of the Plexiglas chamber for extracellular stimulation (Fig. 1*A*). The electrodes were not in direct contact with the cells (an estimated distance of 250–280 μm) but stimulated a small myocyte cluster immediately beneath them, initiating a wave of $[Ca^{2+}]_i$ transients that then spread through the rest of the network (no damage to the stimulated cells, including baseline intracellular Ca^{2+} levels, was detected). Specifically, monophasic 1.2-ms pacing pulses were applied starting at a pacing voltage of 0.4 V/cm (the distance between electrodes was 1 mm) and then increased in 0.1-V increments until each pacing impulse was followed by a recorded $[Ca^{2+}]_i$ wave (average threshold values were 0.8 V/cm). The monolayer was then continuously paced by a voltage 20% higher than the excitation threshold. Viability of monolayers after the experiment was assessed by *1*) their morphology in phase-contrast mode, *2*) spontaneous beating rate, and *3*) permeability to trypan blue. None of these were affected by cell pacing or continuous perfusion with the control Tyrode solution using specified flow rates.

Experimental protocol

Myocytes were superfused with a control Tyrode solution [consisting of (in mM) 136 NaCl, 0.8 $MgCl_2$, 4.0 KCl, 1.2 $CaCl_2$, 5.6 glucose, and 10 HEPES; pH 7.3] through *inlet 1*, and the intracellular Ca^{2+} transients (either paced or spontaneous) were recorded. After 5–10 min, *inlet 2* was opened, and the second solution started to flow over the coverslip, creating a small oval-shaped zone within the larger area of control Tyrode solution (Fig. 2). Unless specified otherwise, the terms “ischemic” or “injury” environment in this study refer to a solution that reproduces certain elements of the extracellular milieu of ischemic cells (38); the injury solution consisted of (in mM) 136 NaCl, 0.8 MgCl, 8 KCl, 1.2 $CaCl_2$, 20 deoxyglucose, 5 HEPES, and 5 MES; pH 6.5. All solutions, including the injury solution, were equilibrated with atmospheric oxygen.

Acquisition system

Fluo 4-loaded cells were imaged with low-power magnification objectives (Olympus UplanApo ×4/0.16NA, PlanApo ×2/0.08NA, and UplanF1 ×10/0.30NA) to capture the injury and control zones simultaneously. The imaging system consisted of an Olympus XL-70 inverted microscope, a Bio-Rad MRC 1024 confocal system, and a 488-nm argon laser for fluo 4 excitation. Because of the confocality of the system, it displays only a thin optical section from the focal plane where the cells are found. High quantum yield of fluo 4 and sequential point-by-point laser scanning of the sample minimizes light exposure and data can be acquire continuously for hours at speeds up to 100 ms/frame without notable cell damage and probe bleaching. Fluorescence intensities from multiple (up to 15) regions of interest were acquired simultaneously, in real time, using a Bio-Rad Lasersharp Time Course module, with a frequency of acquisition ranging from 100 to 200 ms for *x-y* images or 2 ms/line in a line scan mode. Data and images were analyzed using Microcal Origin 4.0 and Scion (National Institutes of Health) Image software.

RESULTS

Shape and stability of local I-zone

The critical issue for this approach was to design a cell superfusion chamber that creates a localized I-zone while keeping neighboring cells under normal conditions. The chamber had to satisfy several criteria: *1*) maintain stable borders of the I-zone during an experiment, *2*) provide a means for relatively fast medium changes (within seconds), *3*) not affect cells by the shear stress imposed by the flow, and *4*) fit on the stage of an inverted microscope. The design shown in Fig. 1, *A* and *B*, meets these requirements and was accomplished by *1*) sequential arrangement of two inlets, *2*) use of a common outlet to insure that differences of inflow rates between the two solutions did not affect stability of the I-zone, and *3*) employment of a multisyringe pump to eliminate flow pulsations associated with peristaltic perfusion. Figure 1*C* shows the shape of the I-zone, which was created on a cell-free coverslip using a 30-ml syringe for the control flow and a 10-ml syringe for injury solution perfusion. The I-zone was demarcated by including 100 nM dichlorofluorescein (DCF) in the second solution. The distribution of DCF fluorescence across the transition zone reveals a sigmoidally shaped intensity profile (Fig. 1*C*). If the border width is defined as the difference between the locations at which the intensity was 10 and 90% of maximum, the average physical border was ~180 μm wide and remained stable during the entire period of superfusion.

Figure 2 illustrates the formation and gradual washout of the I-zone using DCF-containing solution and shows rapid (<15 s) exchange between the injury and control Tyrode solutions. The levels of DCF fluorescence intensity for different areas inside the I-zone are essentially identical and remain stable throughout duration of the injury solution perfusion, which indicates homogeneous superfusion within the I-zone. Linear velocities of the flow within the chamber are ~0.5 mm/s (as determined by including 15-μm fluorescent beads into the solution flowing through the I-zone), and no changes in the peak-to-peak amplitude and frequency of $[Ca^{2+}]_i$ transients occurred when control Tyrode solution was used to superfuse cells through *inlet 2* (data not shown).

Cell monolayer before local injury

After attachment to a laminin substrate, rounded cardiac myocytes spread and form multiple gap junctions with their neighbors (12,16,22). By the third day in culture, these latent pacemaker cells develop uniform rhythmical contractions and express specific cardiac muscle isoforms of myosin light chain kinase-2, β-myosin, sarcomeric α-actin, and tropomyosin (17,39). The percentage of cells positive for sarcomeric myosin in our cultures

exceeded 80%. On *days 3–7*, two-dimensional networks, which contain thousands of spontaneously beating cells with visible striations, functionally and morphologically resemble cardiac muscle tissue (Fig. 3, *A* and *B*). The intrinsic spontaneous activity of the monolayer can be overridden by a faster pace from a distal node, which was created by using a pair of extracellular platinum electrodes imbedded into the plastic top of the chamber and positioned close to the edge of coverslip (Fig. 1*A*). In such experiments, extracellular electrodes excited the group of myocytes directly beneath them. This was followed by the spread of excitation from the stimulated cell cluster to the rest of the network. Each spontaneous or field-stimulated action potential was associated with an increase in cytosolic intracellular Ca^{2+}, which could be recorded as a fluorescent transient in cells loaded with fluorescent calcium indicator (Fig. 3*B*). The experiments were conducted at room temperature, which allowed us to use the temporal resolution of *x-y* mode (100 ms/frame) to reveal the transitional events discussed below, including the formation of clusters at the onset of reperfusion tachycardias, and capture the progression of the wave front during reentry vortexes and ectopic beat generation. Experiments performed at higher temperatures (30 and 37°C) confirmed that the main events observed at 25°C can be reproduced, although temporal resolution of the recordings suffers due to increased beating rate and conduction velocity and shortening of $[Ca^{2+}]_i$ transients. The conduction velocities measured in our cultures were 14–18 cm/s at 37°C and 6–9 cm/s at 25°C (Fig. 3, *C* and *D*). In the *x-y* (100–170 ms/frame) acquisition mode, the cell monolayer appeared as an isotropic field that exhibited rhythmical increases and decreases in fluo 4 fluorescence, as illustrated in Fig. 4, *A* and *B*.

Effects of local injury and border zone effects

During 5-min superfusion with the injury solution, which mimics certain elements of the extracellular environment during ischemia (see MATERIALS AND METHODS), the magnitude of $[Ca^{2+}]_i$ transients within the I-zone progressively declined and was followed by cessation of cell beating (Fig. 4). The effects on the cells within the I-zone were similar when experiments were conducted in spontaneously beating (n = 31) or externally paced cell monolayers (n = 16). No changes in spontaneous beating frequency inside and outside the I-zone were detected before the cessation of cell beating. Cells that have had a diminished amplitude of $[Ca^{2+}]_i$ transients but continued to be excited formed a so-called “functional” border ~0.5 mm wide. To resolve the shapes of intracellular Ca^{2+} transients within individual myocytes in control and border zones, we used a line scan mode of the confocal setup in which data were acquired from ischemic and control zones with high temporal resolution (Fig. 5). The slope of the line, which marks the onset of Ca^{2+} transients (an indicator of impulse conduction velocity), was changed in the I-zone (Fig. 5*B*; dotted line) consistently with decreased cell-to-cell coupling and diminished cell excitability in an ischemic environment (4,23,31).

Reperfusion tachyarrhythmias

On restoration of control flow, two scenarios were observed. In 83% (39 of 47) of the cases, $[Ca^{2+}]_i$ transients gradually returned to the I-zone, leading to a resumption of regular $[Ca^{2+}]_i$ transients throughout the entire field. In 17% (8 of 47) of the cases, however, an immediate tachyarrhythmic response was generated (Fig. 6). Such transient tachyarrhythmias ranged from 20 to 100 s (88 ± 26 s) and were associated with a ~70% increase in average beating frequency (from 0.29 ± 0.04 to 0.49 ± 0.05 Hz). The origin of reperfusion tachyarrhythmias was usually a cell or cell cluster within the former I-zone or its borders. After washout, such cell clusters became a center of ectopic activity, the frequency of which exceeded that of $[Ca^{2+}]_i$ transients in the control zone, leading to reperfusion tachyarrhythmias.

Effect of uncouplers and spatiotemporal sequence of reperfusion events

Accumulation of free fatty acids, e.g., arachidonic and palmitoleic acids, in the extracellular milieu of ischemic tissue has been shown previously (10,25). Direct inhibitory effects of these compounds on gap junctional permeability, including halting of impulse propagation in cultured cardiomyocyte monolayers, have been also reported (7,27,40). When we added the gap junction uncoupler heptanol (1 mM) to the injury solution, the incidence of reperfusion arrhythmias sharply increased to 83% (n = 18). Such tachyarrhythmias ranged from 15 s to 3 min (63 ± 12 s) and were associated with a twofold increase in average beating frequency (from 0.30 ± 0.03 to 0.57 ± 0.04 Hz). Inclusion of heptanol in the injury solution also sharpened the appearance of the I-zone due to the narrowing of its functional border by fourfold (Fig. 7). Reperfusion tachyarrhythmias after superfusion with heptanol-containing injury solution were associated with multiple ectopic foci that originated mostly on the border between ischemic and control zones and created a heterogeneous activation pattern (Fig. 8). Opposing waves from different ectopic centers collided and reexcited neighboring areas, and the exact pattern changed rapidly (Fig. 8, *A* and *B*). Within 20–40 s after initiation of reperfusion, a dominant ectopic node was often established (Fig. 8*C*), followed by a restoration of the original propagation pattern in which a $[Ca^{2+}]_i$ transient wave spreads from either the distal cell cluster or pacing electrode through the rest of the network.

DISCUSSION

At present, the numerous investigations that address the mechanisms of ischemia-reperfusion-induced arrhythmias fall into four major groups: *1*) single cell studies (23,38); *2*) mathematical modeling (1,31,33,41); *3*) optical mapping or electrical recording of action potential propagation from the whole heart (19,24); and *4*) use of cardiac fibers to address the origin of border zone arrhythmias (5,18). With the exception of the work by Kleber and colleagues (12,13,27) and the observation of spontaneous rotors in chick myocyte cultures (6), multicellular networks of cultured myocytes remain to be explored as a tool to address the origins of ischemia-reperfusion arrhythmias. At the same time, a multitude of studies (4,23,25,36–38) have addressed the effects of ischemic conditions on primary cultures of neonatal myocytes and freshly isolated cells from adult hearts. In such preparations, a hypoxic/anoxic, hyperkalemic, or acidic environment is applied to the entire sample (either to a coverslip or vial), and a variety of biochemical indices such as lactate dehydrogenase release, lipid peroxidation, permeability to trypan blue, or changes in action potential properties are measured. However, because arrhythmias are often the consequences of structural and functional inhomogeneities (34,40), they cannot be adequately studied in experiments when all cells are subjected to the same environment.

The new approach described in this study was accomplished by bringing together three essential components: *1*) a monolayer of neonatal cardiomyocytes, *2*) a custom-designed perfusion chamber, and *3*) imaging of Ca^{2+} transients. Below is a brief account of these protocols.

A monolayer of neonatal cardiomyocytes possesses many features of cardiac muscle tissue, and recent studies (8,26) revealed that grafts from neonatal cells can be incorporated into a working adult heart. The degree of cell-to-cell coupling and velocity of conduction can be manipulated by three independent means: *1*) age of the primary culture (connexin43 expression has been shown to increase in a time-dependant fashion; see Ref. 22); *2*) plating density of the cells (due to the plasticity of neonatal cells, they are able to stretch and form cell-to-cell contacts within a broad range of seeding concentrations); and *3*) altering the myocyte-to-fibroblast ratio (12).

To create a temporally and spatially stable local area of injury within a two-dimensional cellular network, we modified earlier designs of dual-perfusion chambers, where parallel streams were used to create two separate environments (3) or study border zone events (15). The width of the I-zone can be modulated in a range of 1–4 mm by varying the perfusion rate through the inlets, and the length of the zone can be modified by positioning *inlet 2* closer to the outlet (Fig. 1*B*). Stimulating electrodes, temperature, pH, or other mini-probes can be mounted into the plastic top of the chamber. The suggested design allows one to *1*) address the effects of "local injury" and *2*) immediately restore control flow for reperfusion assessment. Both these features are not possible by a parallel stream approach. Furthermore, because "injury loci" simulates an in vivo situation in which a small area of the injured myocardium is surrounded by normally perfused tissue, it should allow us to study impulse propagation around the I-zone, namely, reentry (2).

To monitor propagation of $[Ca^{2+}]_i$ transients, we used the Ca^{2+}-sensitive indicator fluo 4 (dissociation constant = 345 nM). The large signal-to-noise ratio allowed us to employ the lowest intensity of exciting light, and samples were routinely scanned for hours without significant photobleaching or other adverse effects on the cells. Our choice to follow Ca^{2+} transients instead of monitoring action potentials with the use of potentiometric dyes was mainly due to the well-known problems associated with voltage-sensitive indicators. Specifically, low signal-to-noise ratio (4–7% change associated with action potential as compare to manifold change in fluo 4 intensity associated with intracellular Ca^{2+} transient) requires strong illumination to increase optical output. This in turn increases the phototoxicity of the probe, which poisons the cells and causes rapid dye photobleaching (28). Motion artifacts represent another problem and require either application of the electromechanical uncoupler 2,3-butanedione monoxime, which has several side effects (30), or extensive spatial averaging (28). Altogether, these technical issues make currently available potentiometric dyes limited to short experiments in which special arrays of photo sensors are used (13,28). In contrast, calcium dyes are stable and relatively nontoxic, with high quantum yield, which allows for using them in a variety of fluorescence imaging systems (2,4,6,37).

The observed $[Ca^{2+}]_i$ transients are associated with myocyte action potentials, either spontaneous or paced induced (6,13,16,37). Although under certain conditions $[Ca^{2+}]_i$ transients can be dissociated from transmembrane potential changes (e.g., administration of electromechanical uncouplers), generally $[Ca^{2+}]_i$ transients immediately follow transmembrane potential upstroke. A recent study (13) that employed double-stained neonatal myocyte cultures reported a 5.3 ± 1-ms delay between $[Ca^{2+}]_i$ transients and the upstroke of the action potential.

The experiments were conducted at room temperature, at which propagation velocity on control monolayer ranged from 6 to 9 cm/s (Fig. 3*C*). At 37°C, the conduction velocity increased to 14–18 cm/s (Fig. 3*D*). These numbers are similar to the velocity reported by other groups (8,11) who employed neonatal cell cultures. These values are expectedly lower than the reported velocity in the intact neonatal ventricle (25–30 cm/s), due to the larger surface-to-volume ratio and lower degree of electrical coupling in cultured monolayers (8,35). The higher values of conduction velocity observed in other studies (12,13) are likely be due to the differences in isolation procedure, media and culture conditions, plating density of the cells, coverglass coating protocol, or rat strain.

On administration of the injury solution the magnitude of $[Ca^{2+}]_i$ transients inside the I-zone was rapidly suppressed, which led to a cessation of cell beating (Fig. 4). Such an effect was expected due to the direct effects of the injury solution (4,23), which had a low pH (6.5), was lightly hyperkalemic (8 mM), and contained 20 mM deoxyglucose, an inhibitor of

glycolysis (cultured neonatal rat myocytes exhibit a high rate of glycolysis and a low level of oxidative phosphorylation; see Ref. 4). More surprising was the observation that often only a few minutes of perfusion with injury solution (Fig. 6) was sufficient to initiate tachyarrhythmias upon reperfusion. The source of rapid ectopic activity was an individual myocyte or small cell cluster within the former border or I-zone from which the wave activity spread through the entire network. Because of the intrinsic pacemaker activity of neonatal myocytes, observed tachycardias are likely to be a direct effect of the increased depolarization rates of the cell. This, in turn, can be caused by a multitude of factors, including elevation of $[Ca^{2+}]_i$ and intracellular Na^+ concentration, decrease in the intracellular pH, depletion of ATP, and alterations in inward/outward currents, which bring the cell closer to its depolarization threshold (4,31). Similar factors increase the probability of either abnormal automaticity or triggered activity in ventricular and atrial cells (1,18,41). The ability of the method to identify ectopic loci can help to reveal the exact mechanisms of ectopic tachyarrhythmias because specific inhibitors can be readily included in ischemic or reperfusion solutions to test the contribution of the above factors. The focal mechanisms are reportedly responsible for initiation of up to 70% of ventricular tachycardias, albeit the relative importance of the ectopic and reentry type of arrhythmias associated with reperfusion of the ischemic myocardium remains controversial (5,19,24).

The presence of heptanol sharply increased the incidence of reperfusion arrhythmias and revealed multiple clusters of asynchronously beating cells within the former I-zone (Fig. 8). Even though heptanol has been reported to affect potassium and sodium currents (20,21), the concentration used in our study has been shown to alter primarily intercellular coupling in monolayers of cultured myocytes from neonatal rats (16). The proarrhythmic activity of heptanol and other uncouplers is a well-known phenomenon and generally attributed to slower conduction rates, leading to an increased incidence of unidirectional propagation and reentry tachycardias (9,10,31). The observed increase in ectopic activity associated with the presence of uncoupler in injury solution suggests yet another possible mechanism. Specifically, after removal of heptanol, the gap junction conductance of neonatal myocyte monolayers is restored gradually (16); therefore, cells in the former ischemic I-zone continue to have an impaired coupling with their neighbors. Apparently, the combination of increased excitability and decreased cell-to-cell coupling lessens the dissipation of the charge required for generation of an action potential, increasing the incidence of ectopic tachycardias. The effect is similar to a paradoxical increase in safety factor of impulse propagation in the presence of uncoupler shown in patterned myocytes strands (27) and is due to an increase in the current-to-sink ratio. Accumulation of “physiological” uncouplers, such as palmitoleic and arachidonic acid, has been reported in ischemic cardiac tissue (7,10,16) and may produce similar effects.

Future applications of the described chamber and localized injury approach are not limited to studies of arrhythmia or to monolayers of cardiomyocytes. They can also be used to mimic the effects of localized pharmacological treatments, hormone stimulation, pH changes, or ischemic injury on a confluent cell layer of any origin. The method can be used in single cell experiments to acquire signals from control and treated cells simultaneously, thereby eliminating multiple artifacts associated with coverslip-to-coverslip variability. For example, by plating cells at low densities to preclude cell-to-cell interactions in two distinct environments, one can collect signals simultaneously from nontreated and treated cells (I-zone now being superfused with a drug of choice). Another possible application of the developed approach is that rhythm and conduction disturbances associated with ischemia and reperfusion could be studied in cell networks that have altered expression of connexins or ion channels. This could be achieved with antisense oligodeoxynucleotides, cultures of myocytes from transgenic mice, or by adenovirus-mediated gene expression.

In summary, this study describes a novel experimental approach that recreates ischemia-reperfusion arrhythmias in cellular preparations. The method reveals spatiotemporal changes in a beating behavior induced by a local ischemia-like injury and can be used as an in vitro tool to address the origins of ischemia-reperfusion arrhythmias and test currently available and anticipated antiarrhythmic protocols.

Acknowledgments

The authors are grateful to Drs. Richard Nathan and Sergey Karpinski-Viatchenko for invaluable discussions.

This work was supported in part by National Heart, Lung, and Blood Institute Grant HL-62419.

References

1. Abramovich-Sivan S, Akselrod S. Simulation of atrial activity by a phase response curve based model of a two-dimensional pacemaker cells array: the transition from a normal activation pattern to atrial fibrillation. Biol Cybern 1999;80:141–153. [PubMed: 10074692]
2. Arutunian A, Webster D, Swift L, Sarvazyan N. A new experimental model to emulate ischemia-reperfusion arrhythmias in monolayers of cultured cardiomyocytes (Abstract). Biophys J 2000;78:454A.
3. Atsma DE, Bastiaanse EM, Ince C, van der Laarse A. A novel two-compartment culture dish allows microscopic evaluation of two different treatments in one cell culture simultaneously. Influence of external pH on Na^+/Ca^{2+} exchanger activity in cultured rat cardiomyocytes. Pflügers Arch 1994;428:296–299.
4. Barrigon S, Wang SY, Ji X, Langer GA. Characterization of the calcium overload in cultured neonatal rat cardiomyocytes under metabolic inhibition. J Mol Cell Cardiol 1996;28:1329–1337. [PubMed: 8782074]
5. Boersma L, Brugada J, Kirchhof C, Allessie M. Entrainment of reentrant ventricular tachycardia in anisotropic rings of rabbit myocardium. Mechanisms of termination, changes in morphology, and acceleration. Circulation 1993;88:1852–1865. [PubMed: 8403331]
6. Bub G, Glass L, Publicover NG, Shrier A. Bursting calcium rotors in cultured cardiac myocyte monolayers. Proc Natl Acad Sci USA 1998;95:10283–10287. [PubMed: 9707639]
7. Burt JM, Massey KD, Minnich BN. Uncoupling of cardiac cells by fatty acids: structure-activity relationships. Am J Physiol Cell Physiol 1991;260:C439–C448.
8. Bursac N, Papadaki M, Cohen RJ, Schoen FJ, Eisenberg SR, Carrier R, Vunjak-Novakovic G, Freed LE. Cardiac muscle tissue engineering: toward an in vitro model for electro-physiological studies. Am J Physiol Heart Circ Physiol 1999;277:H433–H444.
9. Callans DJ, Kieval RS, Hook BG, Moore EN, Spear JF. Effect of coronary perfusion of heptanol or potassium on conduction and ventricular arrhythmias. Am J Physiol Heart Circ Physiol 1992;263:H1382–H1389.
10. Dhein S, Krusemann K, Schaefer T. Effects of the gap junction uncoupler palmitoleic acid on the activation and repolarization wavefronts in isolated rabbit hearts. Br J Pharmacol 1999;128:1375–1384. [PubMed: 10602315]
11. Entcheva E, Lu SN, Troppman RH, Sharma V, Tung L. Contact fluorescence imaging of reentry in monolayers of cultured neonatal rat ventricular myocytes. J Cardiovasc Electrophysiol 2000;11:665–676. [PubMed: 10868740]
12. Fast VG, Darrow BJ, Saffitz JE, Kleber AG. Anisotropic activation spread in heart cell monolayers assessed by high-resolution optical mapping. Role of tissue discontinuities. Circ Res 1996;79:115–127. [PubMed: 8925559]
13. Fast VG, Ideker RE. Simultaneous optical mapping of transmembrane potential and intracellular calcium in myocyte cultures. J Cardiovasc Electrophysiol 2000;11:547–556. [PubMed: 10826934]
14. Grant AO. Mechanisms of action of antiarrhythmic drugs: from ion channel blockage to arrhythmia termination. Pacing Clin Electrophysiol 1997;20:432–444. [PubMed: 9058847]

15. Hyatt CJ, Lemasters JJ, Muller-Borer BJ, Johnson TA, Cascio WE. A superfusion system to study border zones in confluent cultures of neonatal rat heart cells. Am J Physiol Heart Circ Physiol 1998;274:H2001–H2008.
16. Kimura H, Oyamada Y, Ohshika H, Mori M, Oyamada M. Reversible inhibition of gap junctional intercellular communication, synchronous contraction, and synchronism of intracellular Ca^{2+} fluctuation in cultured neonatal rat cardiac myocytes by heptanol. Exp Cell Res 1995;220:348–345. [PubMed: 7556443]
17. Luther HP, Hille S, Haase H, Morano I. Influence of mechanical activity, adrenergic stimulation, and calcium on the expression of myosin heavy chains in cultivated neonatal cardiomyocytes. J Cell Biochem 1997;64:458–465. [PubMed: 9057103]
18. Maldonado C, Li ZY, Wead WB, Szabo T, Kupersmith J. Mechanisms of triggered activity induction at the border zone of normal and abnormal cardiac tissue. J Electrocardiol 1996;29:309–318. [PubMed: 8913905]
19. Mandapati R, Skanes A, Chen J, Berenfeld O, Jalife J. Stable microreentrant sources as a mechanism of atrial fibrillation in the isolated sheep heart. Circulation 2000;101:194–199. [PubMed: 10637208]
20. Nelson WL, Makielski JC. Block of sodium current by heptanol in voltage-clamped canine cardiac Purkinje cells. Circ Res 1991;68:977–983. [PubMed: 1849060]
21. Niggli E, Rudisuli A, Maurer P, Weingart R. Effects of general anesthetics on current flow across membranes in guinea pig myocytes. Am J Physiol Cell Physiol 1989;256:C273–C281.
22. Oyamada M, Kimura H, Oyamada Y, Miyamoto A, Ohshika H, Mori M. The expression, phosphorylation, and localization of connexin 43 and gap-junctional intercellular communication during the establishment of a synchronized contraction of cultured neonatal rat cardiac myocytes. Exp Cell Res 1994;212:351–358. [PubMed: 8187829]
23. Pierce GN, Czubryt MP. The contribution of ionic imbalance to ischemia/reperfusion-induced injury. J Mol Cell Cardiol 1995;27:53–63. [PubMed: 7760373]
24. Pogwizd SM, Hoyt RH, Saffitz JE, Corr PB, Cox JL, Cain ME. Reentrant and focal mechanisms underlying ventricular tachycardia in the human heart. Circulation 1992;86:1872–1887. [PubMed: 1451259]
25. Post JA, Verkleij AJ, Langer GA. Organization and function of sarcolemmal phospholipids in control and ischemic/reperfused cardiomyocytes. J Mol Cell Cardiol 1995;27:749–760. [PubMed: 7776380]
26. Reinecke H, Zhang M, Bartosek T, Murry CE. Survival, integration, and differentiation of cardiomyocyte grafts: a study in normal and injured rat hearts. Circulation 1999;100:193–202. [PubMed: 10402450]
27. Rohr S, Kucera JP, Fast VG, Kleber AG. Paradoxical improvement of impulse conduction in cardiac tissue by partial cellular uncoupling. Science 1997;275:841–844. [PubMed: 9012353]
28. Rohr S, Salzberg BM. Multiple site optical recording of transmembrane voltage (MSORTV) in patterned growth heart cell cultures: assessing electrical behavior, with microsecond resolution, on a cellular, and subcellular scale. Biophys J 1994;67:1301–1315. [PubMed: 7811945]
29. Sarvazyan N. An alternative preconditioning mechanism? J Mol Cell Cardiol 1998;30:2785–2786. [PubMed: 9990548]
30. Sellin LC, McArdle JJ. Multiple effects of 2,3-butanedione monoxime. Pharmacol Toxicol 1994;74:305–313. [PubMed: 7937562]
31. Shaw RM, Rudy Y. Electrophysiologic effects of acute myocardial ischemia. A mechanistic investigation of action potential conduction and conduction failure. Circ Res 1997;80:124–138. [PubMed: 8978331]
32. Spach MS, Miller WT, Geselowitz DB, Barr RC, Kootsey JM, Johnson EA. The discontinuous nature of propagation in normal canine cardiac muscle. Evidence for recurrent discontinuities of intracellular resistance that affect the membrane currents. Circ Res 1981;48:39–54. [PubMed: 7438345]
33. Starmer CF, Biktashev VN, Romashko DN, Stepanov MR, Makarova ON, Krinsky VI. Vulnerability in an excitable medium: analytical and numerical studies of initiating unidirectional propagation. Biophys J 1993;65:1775–1787. [PubMed: 8298011]

34. Strauss, HC. Perspective and future directions: arrhythmias and discontinuous conduction. In: Spooner, PM.; Joyner, RW.; Jalife, J., editors. Discontinuous Conduction in the Heart. Armonk, NY: Futura; 1997. p. 547-550.

35. Sun LS, Legato MJ, Rosen TS, Steinberg SF, Rosen MR. Sympathetic innervation modulates ventricular impulse propagation and repolarisation in the immature rat heart. Cardiovasc Res 1993;27:459–463. [PubMed: 8490947]

36. Thandroyen FT, Bellotto D, Katayama A, Hagler HK, Willerson JT, Buja LM. Subcellular electrolyte alterations during progressive hypoxia and following reoxygenation in isolated neonatal rat ventricular myocytes. Circ Res 1992;71:106–119. [PubMed: 1606659]

37. Thandroyen F, Morris AC, Hagler HK, Ziman B, Pai L, Willerson JT, Buja LM. Intracellular calcium transients and arrhythmia in isolated heart cells. Circ Res 1991;69:810–819. [PubMed: 1873874]

38. VandenHoek TL, Shao Z, Li C, Zak R, Schumacker PT, Becker LB. Reperfusion injury in cardiac myocytes after simulated ischemia. Am J Physiol Heart Circ Physiol 1996;270:H1334–H1341.

39. Webster DR. Neonatal rat cardiomyocytes possess a large population of stable microtubules that is enriched in post-translationally modified subunits. J Mol Cell Cardiol 1997;29:2813–2822. [PubMed: 9344775]

40. Wolk R, Cobbe SM, Hicks MN, Kane KA. Functional, structural, and dynamic basis of electrical heterogeneity in healthy and diseased cardiac muscle: implications for arrhythmogenesis and anti-arrhythmic drug therapy. Pharmacol Ther 1999;84:207–231. [PubMed: 10596907]

41. Zeng J, Rudy Y. Early afterdepolarizations in cardiac myocytes: mechanism and rate dependence. Biophys J 1995;68:949–964. [PubMed: 7538806]

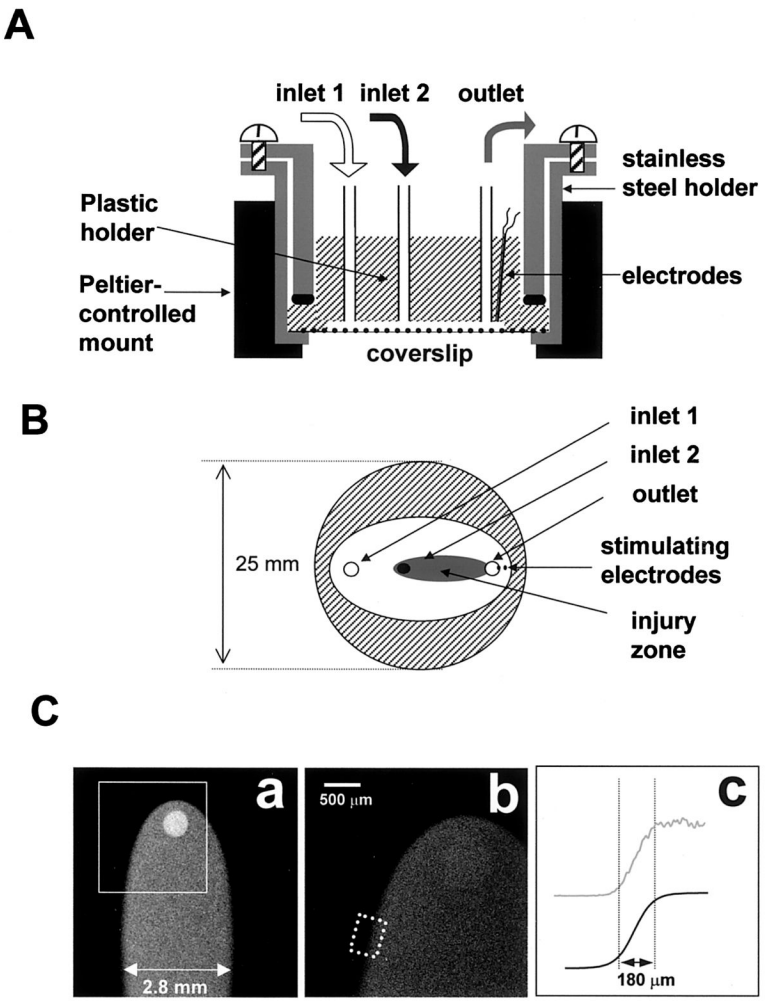

Fig. 1.

Diagram of the superfusion chamber. *A*: cross section. Solutions are delivered to two inlets by an automated multisyringe pump. The chamber is placed inside a Peltier temperature-controlled mount, and cells are observed in an inverted mode using a Bio-Rad 1024 MRC confocal imaging system. *B*: bottom view. Only the plastic holder and coverslip are shown. Injury zone (I-zone) is depicted (shaded area). *C*: I-zone. The shape of an I-zone created on a cell-free coverslip by superfusion with dichlorofluorescein (DCF)-containing solution (*a*: ×2 objective; *b*: ×4 objective). In *c*, the *top curve* (gray line) illustrates the profile of mean fluorescence intensity across the border zone (dotted rectangle in *b*), the *bottom curve* (solid line) is its sigmoid fit (border zone width was defined as the distance between 10 and 90% of the curve maximum intensity).

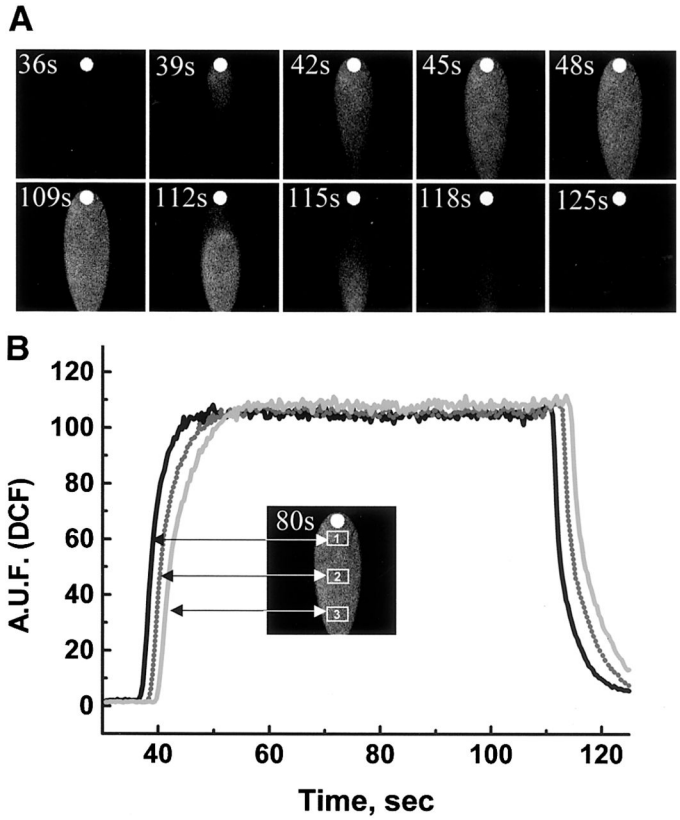

Fig. 2.

Formation and washoff of the I-zone. *A*: images are composed from sequential 3-s frames acquired during formation (*top*) and washoff (*bottom*) of the I-zone created on a cell-free coverslip by superfusion with DCF-containing injury solution (×2 objective). *B*: 3 traces shown correspond to rectangular regions within the I-zone (*inset*) and illustrate the homogeneity and stability of the environment within the I-zone. AUF, arbitrary units of fluorescence.

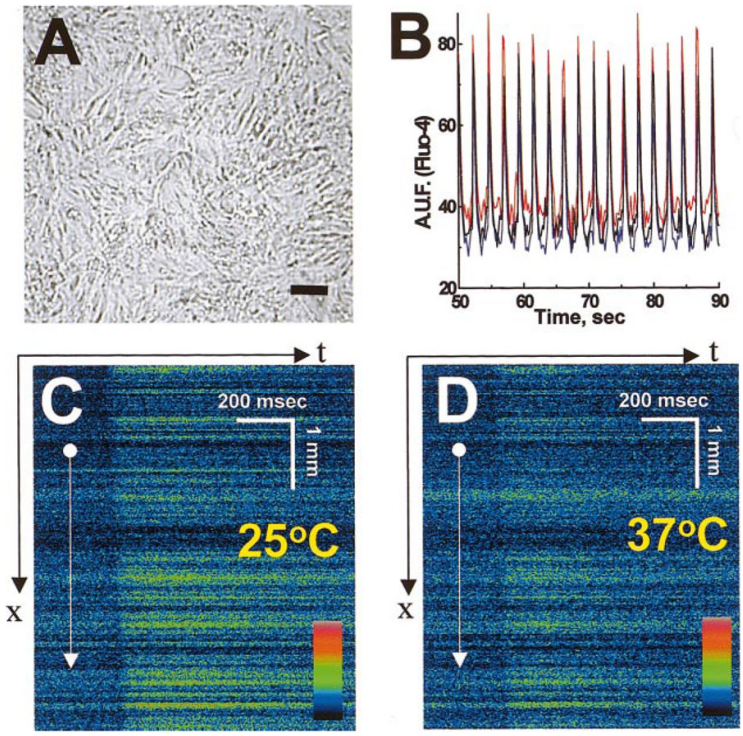

Fig. 3.

Basic features of cultured cardiomyocyte networks. *A*: phase-contrast image of isotropic cardiomyocyte culture. Bar = 100 μm. *B*: cell beating as recorded using fluo 4-loaded cells. Traces represent intracellular Ca^{2+} transients recorded from three regions of interests (blue, red, and black). *C* and *D*: velocity of impulse propagation. In *x*-*t* mode, fluorescence intensity values are collected along a fixed *x* line every 2 ms and the lines are plotted sequentially, forming a *x*-*t* image. If the *x* line is positioned perpendicularly to the front of propagating calcium wave, the speed of the wave (d*x*/d*t*) can be derived from the slope of the line, which marks the upstroke of Ca^{2+} transients. The images show an action potential-induced calcium wave recorded at 25°C with a propagation speed of 9 cm/s (*C*) and at 37°C with propagation speed of 15 cm/s (*D*).

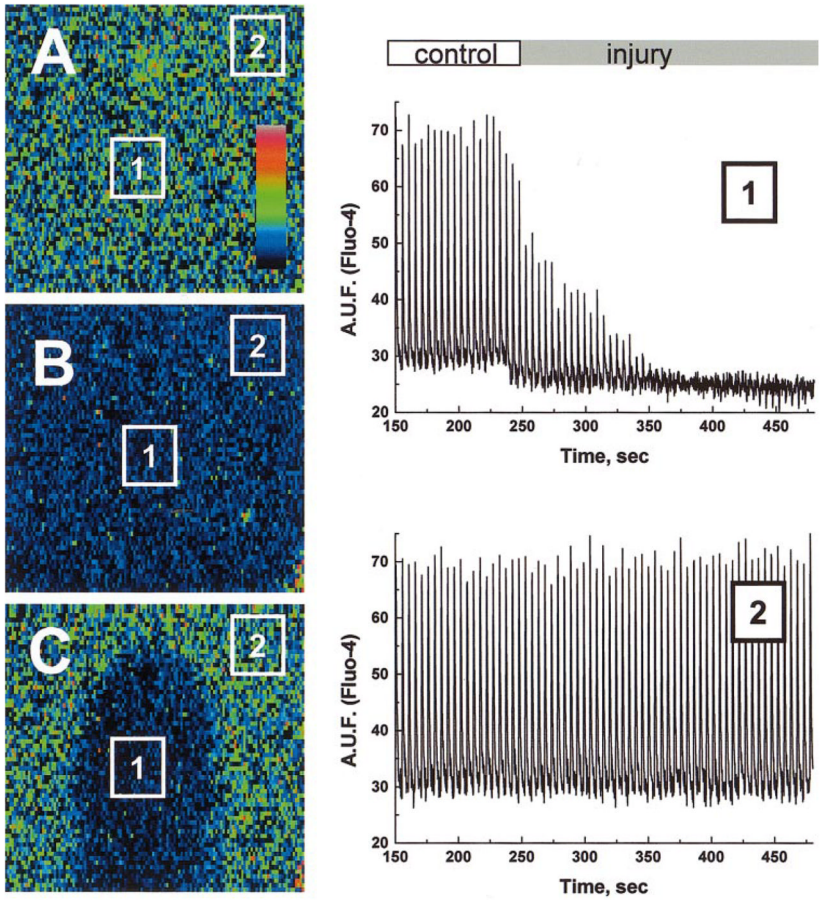

Fig. 4.

Appearance of ischemic I-zone within a monolayer of neonatal myocytes. The images illustrate the appearance of a monolayer before (*A* and *B*) and after 5 min of local injury (*C*). Because of the high degree of cell-to-cell coupling, the whole field alternates between a high intensity "systolic" state (*A*) and a low intensity "diastolic" state (*B*). The suppression of intracellular Ca^{2+} concentration ($[Ca^{2+}]_i$) transients in the I-zone is particularly evident during systole (*C*). Low spatial resolution of the images is due to the fast scanning required to capture the whole field during a single state. At this magnification, each of 128 × 128 pixels corresponds to a square of 44 μm on each side. In this and other figures, pseudocolor refers to relative $[Ca^{2+}]_i$. Two representative $[Ca^{2+}]_i$ traces are shown: one from rectangular area inside the I-zone (*1*) and one from the rectangular area outside the I-zone (*2*).

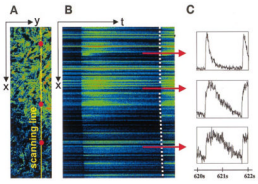

Fig. 5.

Assessment of intracellular Ca^{2+} transients during ischemia. *A: x-y* image of border area of I-zone. Yellow line, position of the laser beam for the *x-t* scanning. *B: x-t* image (sample was scanned every 2 ms along the line placed across the I-zone). Each intracellular Ca^{2+} transient is reflected as a "flash" along the line. *C*: post acquisition analysis of *x-t* images allows one to extract high temporal resolution traces for each cell positioned along the line. Three red dots placed on the top of the *x-y* image (*A*) and three red lines positioned along corresponding areas of *x-t* image (*B*) designate approximate positions of cells for which intracellular Ca^{2+} transients are shown. The slope of the line, which marks the upstroke of intacellular Ca^{2+} transients (dotted line), shows a slowing of impulse conduction in the I-zone.

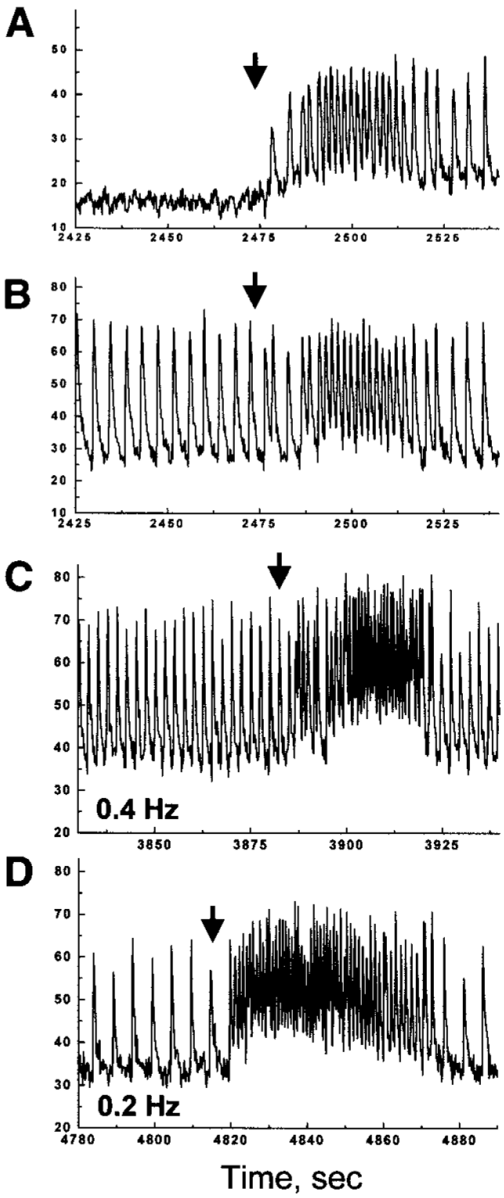

Fig. 6.

Reperfusion arrhythmias in spontaneously beating and paced cells monolayers. *A* and *B*: representative traces collected from the I-zone (*A*) and control area (*B*) during injury and subsequent reperfusion. The experiment was conducted in a spontaneously beating cell monolayer. *C* and *D*: representative traces acquired from the control area during injury and subsequent reperfusion of the monolayer paced at 0.4 (*C*) and 0.2 Hz (*D*). On restoration of the control Tyrode solution (arrows), rapid ectopic activity within the former I-zone overrode external stimulation, leading to a transient tachycardia encompassing the entire network.

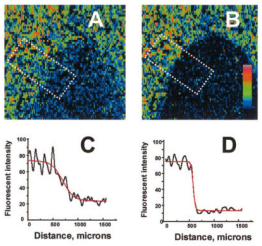

Fig. 7.

Narrowing of functional borders of the I-zone in the presence of an uncoupler. *A*: appearance of the I-zone after 3 min of perfusion with injury solution. *B*: appearance of the I-zone after 3 min of perfusion with injury solution containing 1 mmol/l heptanol. *C* and *D*: maximum intensity of $[Ca^{2+}]i$ transients across the border was used to reveal the width of the functional border zone. The values of maximum fluo 4 intensity associated with high systolic intracellular Ca^{2+} levels were fitted into a sigmoidal curve, and border width was determined as the distance between 10 and 90% of the curve maximum intensity. The functional border zone was 120 ± 8 μm in the presence of 1 mM heptanol in injury solution (*D*) compared with 473 ± 51 μm without the uncoupler (*C*) (means ± SD, $n = 4$).

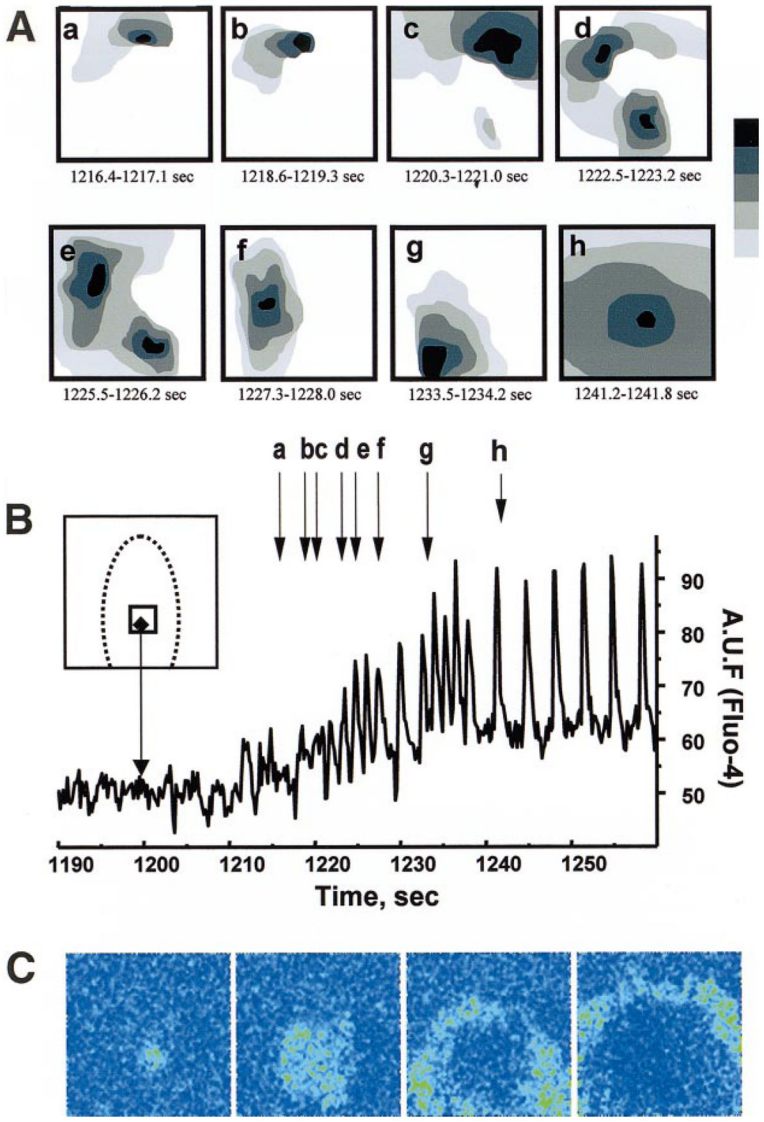

Fig. 8.

Origin and spatiotemporal pattern of reperfusion arrhythmias. *A*: gray scale-coded diagrams represent isochronal maps, which illustrate the formation of multiple ectopic clusters on removal of heptanol-containing injury solution. For clarity only, a few episodes are shown. Five scans were used to compose each diagram using $[Ca^{2+}]i$ transient wave fronts. The gray scale extends from 0 (black) to 700 ms (light gray). Note the formation of multiple ectopic loci on a border of the former I-zone (*a–g*) followed by a dominant ectopic (*h*) emanating from the former I-zone. *B*: trace collected from rectangular box inside the I-zone (*inset*). Vertical arrows indicate the corresponding isochronal maps shown in *A. C*: four temporal derivatives (dF/d*t*) for five sequential frames, which illustrate propagation from the dominant ectopic shown. These images are similar to images produced by activation isochrones but do not require any assumption about what constitutes a local activation.